Period-doubling scenario and crisis-induced intermittency in natural convection between two vertical differentially heated plates

Zhenlan Gao[a,b], Bérengère Podvin[a], Anne Sergent[a,b], Shihe Xin[c], Patrick Le Quéré[a]

a. *CNRS, LIMSI, UPR3251, BP 133, 91403, Orsay Cedex, France*
b. *Universite Pierre et Marie Curie-Paris 6, 4, Place Jussieu, 75252 Paris, Cedex 05, France*
c. *CETHIL, INSA de Lyon, 69621 Villeurbanne Cedex, France*

Résumé :

Nous étudions la transition vers le chaos de l'écoulement d'air entre deux plaques verticales differentiellement chauffées. Le domaine bi-périodique de simulation est restreint à de petites longueurs de périodicité. Le comportement spatio-temporel de l'écoulement en fonction du nombre de Rayleigh (Ra) est étudié par simulation numérique directe 3D (DNS). La route vers le chaos se fait par une cascade de bifurcations sous-harmoniques. Des fenêtres de régimes multi-périodiques et une crise d'élargissement de l'attracteur sont également observées. Quand Ra augmente, une intermittence se produit correspondant à une crise par fusion de deux attracteurs. Pour des valeurs de Ra supérieures, une fenêtre périodique apparaît, suivie ensuite d'un retour à un régime chaotique et intermittent.

Abstract :

The chaotic regime of the natural convection of air between two vertical plates maintained at different temperatures is studied. The periodic dimensions of the plates are relatively small. Direct numerical simulation (DNS) is used to study the spatio-temporal behavior of the flow, as the Rayleigh number (Ra) increases. The flow becomes temporally chaotic through a period-doubling cascade. Chaos then becomes more developed, and windows of multi-periodic regimes, crises are observed. As the Rayleigh is further increased, intermittency is observed, and is seen to correspond to an "attractor-merging" crisis. For still higher values of Ra, a periodic regime is observed, which then gives way to a fully chaotic and intermittent regime.

Mots clefs : natural convection ; period-doubling scenario ; crisis-induced intermittency

1 Introduction

The flow between two vertical differentially heated plates can be considered as a simplified model for a number of industrial applications, such as the double-panned windows, heat exchangers in the reactors. Transition to chaos of the flow in this configuration has been studied by analytical, experimental, and numerical means since Batchelor's pioneering work[1]. Most analyses have been carried out in the 2D configurations[2, 3]. Some 3D studies[4, 5] have been limited to the first few instabilities, when the Rayleigh number remains close to its critical value. We have recently begun an investigation of this problem using 3D DNS, where only the dependence of air flow on Ra is considered[6]. It has been observed that although the first instability of the flow is 2D and steady, the steady flow rapidly becomes 3D, through a second supercritical pitchfork bifurcation. The flow structures observed consist of (i) primary rolls which are deformed in the transversal directions, (ii) braids or counter-rotating vortices playing the role to link the primary rolls, and (iii) two small counter-rotating vortices inside each primary rolls as shown in Figure 1 (b). After a supercritical Hopf bifurcation, the 3D flow

becomes oscillatory. A significant exchange of vorticity is detected between the primary rolls and braids, which are oscillating out of phase. When the computational domain accommodates only one primary roll in the vertical direction, a cascade of period-doubling bifurcations is observed as the Rayleigh number increases, and eventually leads to temporally chaotic flow. For larger domains, this behavior is superseded by a spatial modulation instability in the vertical direction. In the present paper, we will focus on the case of a small domain. Similar behavior have been reported in 2D for laterally heated cavities, as in the case of a vibrational cavity heated from the sides [7], where a subharmonic cascade, followed by a Pomeau-Manneville type-I intermittency was observed. Chaos has also been observed in 3D cavities at much higher Rayleigh numbers $Ra > 10^8$ [8, 9, 10]. We note that in our case, periodic boundary conditions in the vertical direction replace horizontal wall boundary conditions. We first describe the numerical configuration, then show simulation results.

2 Physical model and numerical methods

We consider the flow of air between two infinite vertical plates maintained at different temperatures. The configuration is represented in Figure 1. The distance between the two plates is D, and the period height and depth of the plates are L_z and L_y respectively. The temperature difference between the two plates is ΔT. The direction x is normal to the plates, the transverse direction is y, and the gravity g is opposite to the vertical direction z.

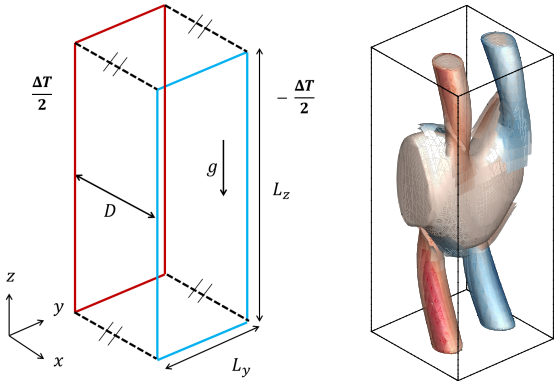

(a) (b)

FIGURE 1 – (a) Study domain (b) Q-criterion visualization of flow structure at $Ra = 11500$, $Q = 0.12$

The fluid properties of air are the kinetic viscosity ν, thermal diffusivity κ, and thermal expansion coefficient β. Four nondimensional parameters characterizing the flow are chosen in the following way : the Prandtl number $Pr = \dfrac{\nu}{\kappa}$, the Rayleigh number based on the width of the gap between the two plates $Ra = \frac{g\beta\Delta T D^3}{\nu\kappa}$, and the transverse and vertical aspect ratio $A_y = L_y/D$ and $A_z = L_z/D$, respectively. Only the Rayleigh number is varied in the present study. The Prandtl number of air is fixed to 0.71. The transverse aspect ratio is set to be $A_y = 1$, the vertical aspect ratio is set to $A_z = 2.5$, which corresponds to the critical wavenumber $k_c \sim 2\pi/2.5$ obtained by the stability analysis[2, 3, 6].

2.1 Equations of motion

The flow is governed by the Navier-Stokes equations within the Boussinesq approximation. D, ΔT, $\kappa\sqrt{Ra}/D$ are chosen as the references for length, temperature and velocity, respectively. The nondimensionalized equations are :

$$\nabla \cdot \vec{u} = 0 \tag{1}$$

$$\frac{\partial \vec{u}}{\partial t} + \vec{u} \cdot \nabla \vec{u} = -\nabla \tilde{p} + \frac{Pr}{\sqrt{Ra}} \Delta \vec{u} + Pr\tilde{\theta}\vec{z} \tag{2}$$

$$\frac{\partial \tilde{\theta}}{\partial t} + \vec{u} \cdot \nabla \tilde{\theta} = \frac{1}{\sqrt{Ra}} \Delta \tilde{\theta} \tag{3}$$

with Dirichlet boundary conditions at the plates

$$\overrightarrow{u}(0,y,z,t) = \overrightarrow{u}(1,y,z,t) = 0, \quad \tilde{\theta}(0,y,z,t) = 0.5, \quad \tilde{\theta}(1,y,z,t) = -0.5 \tag{4}$$

and periodic conditions in the y and z directions. Here t denotes time, $\overrightarrow{u} = (\tilde{u}, \tilde{v}, \tilde{w})$ is the velocity vector, $\tilde{p}$ is the pressure, $\tilde{\theta}$ is the temperature. The equations (1)-(4) admit an $O(2) \times O(2)$ symmetry. One $O(2)$ symmetry corresponds to the translation in the transverse direction y and the reflection $y \to -y$, while the other corresponds to the translations in the vertical direction z and a reflection that combines centrosymmetry and Boussinesq symmetry : $(x, z, T) \to (-x, -z, -T)$.

2.2 Numerical methods

A spectral code [11] developped at LIMSI is used to carry out the simulations. The spatial domain is discretized by the Chebyshev-Fourier collocation method. The projection-correction method is used to enforce the incompressibility of the flow. The equations are integrated in time with a second-order mixed explicit-implicit scheme. A Chebyshev discretization with 40 modes is applied in the direction x, while the Fourier discretization is used in the transverse and vertical directions. 30 Fourier modes are used in the transverse direction y for $A_y = 1$, while 60 Fourier modes are used in the vertical direction z for $A_z = 2.5$. Convergence of the spatial discretization has been established [6]. We run our simulations by following a branch of stable solutions. An instantaneous flow realization in the mono-periodic regime at $Ra = 11300$ is taken as the initial condition for the initial run. For each simulation, the Rayleigh number is increased by small increment of 2, compared to the previous one. The data is sampled when the asymptotic chaotic regime has been reached, that is to say transient effects have faded after long time numerical integrations (about 10^4 nondimensional time units). At the end of each run, the asymptotic solution obtained at a ginve Rayleigh number is used as the initial condition for the simulation at the next higher Rayleigh number.

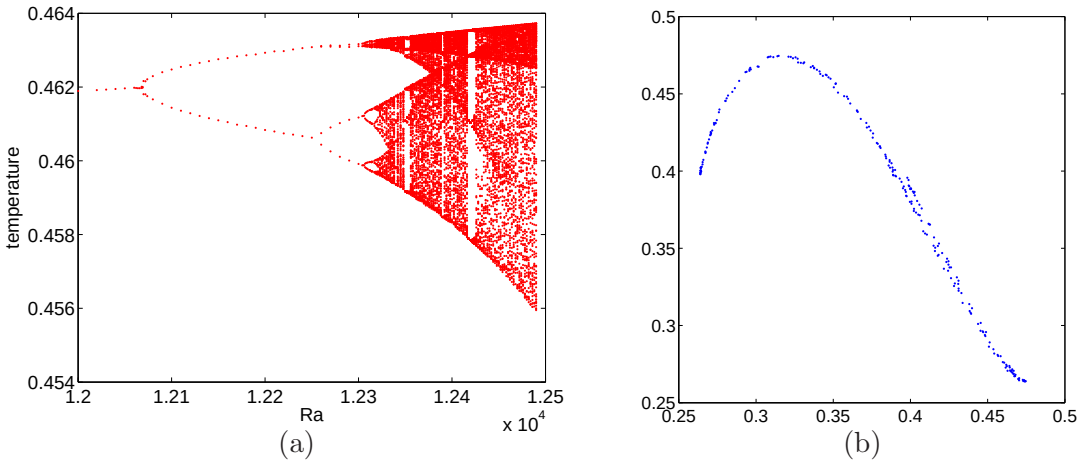

(a) (b)

FIGURE 2 – (a) : bifurcation diagram obtained by using the local maxima of the temperature timeseries at the point (0.038 0.097 0.983). $Ra \in [12000, 12500]$; (b) : first return map obtained by using the local maxima of the Fourier mode $k = 1$ timeseries, calculated from the temperature distribution on the vertical line $x = 0.0381$ and $y = 0.5$.

3 Results

3.1 Period-doubling cascade

After having experienced two supercritical pitchfork bifurcations at $Ra = 5708$ and $Ra = 9980$ through which the flow becomes 2D steady then 3D steady, a supercritical Hopf bifurcation occurs at $Ra = 11270$, as the flow becomes temporally mono-periodic. As the Rayleigh number increases, a sequence of period-doubling bifurcations is observed, which leads to temporal chaotic flow [6]. A bifurcation

TABLE 1 – Summary of period-doubling bifurcations

Bifurcations $2^i \rightarrow 2^{i+1}$	Local critical $Ra_{2^i \rightarrow 2^{i+1}}$	Estimated Feigenbaum constant $\tilde{\delta}$
0-1	11270	
1-2	12068.09	
2-4	12258.42	4.193
4-8	12305.76	4.020
8-16	12316.72	4.321

diagram of Figure 2 (a) is constructed by the using local maxima T_n of the temperature timeseries at the point (0.038 0.097 0.983), which is located in the boundary layer near the hot wall. It is found to be quite similar to that of one-dimensional maps, like the logistic map[13]. 1-D maps with a quadratic maximum are expected to follow a Feigenbaum scenario [12], and this is what we find in the simulation. The local critical Rayleigh numbers $Ra_{2^i \rightarrow 2^{i+1}}$ $(i = 0, 1, 2, 3, ...)$ corresponding to the onset of a 2^i-periodic regime are estimated from linear extrapolation. From these estimations, approximations for the Feigenbaum constant are calculated and listed in Table 1. Some agreement with the theoretical value $\delta = 4.66920161....$ [13] is observed. Using the theoretical value for the Feigenbaum number, the chaotic regime is estimated to be reached around $Ra \sim 12320$. For higher Rayleigh numbers, the chaos continues to develop as shown in the bifurcation diagram. Several periodic windows with numbers of cycles 12, 10, 6, 5, etc, are observed. For example, a large '*period-6* windows' (a *period-3* windows in each band) appears at $Ra = 12350$ in the bifurcation diagram. It then undergoes a period-doubling cascade in which orbits of period 3×2^m are successively produced This cascade once again leads the flow to a chaotic behavior. For still higher Rayleigh numbers, the attractor abruptly widens into two large bandes similar in size to that before the stable '*period-6*' orbit came into existence. Finally, the two large bands merge at around $Ra = 12380$ and form a large single chaotic band. In this chaotic regime, all the points fall on a single curve with 3 branches in the first return map at $Ra = 12380$ as shown in Figure 2 (b), which is similar to the case of Lorenz map [14]. For this range of Ra, the spatial structure remains similar to that observed in the mono-periodic regime[6], but is observed to pulsate in time in a quasi-regular fashion.

3.2 Crisis-induced intermittency

The bifurcation diagram for the range $Ra \in [12400, 12600]$ is represented in Figure 3(a). A rectangular area filled with points abruptly appears on the top-right corner of the figure for $Ra = 12546$, which is the sign of a crisis [15]. Above this Rayleigh number, intermittent behavior is observed, as is indicated in Figure 3 (b) which represents the temporal evolution of the first Fourier mode $k = 1$ of the temperature distribution on the vertical line ($x = 0.0381$ and $y = 0.5$). This evolution is characterized by switches between chaotic states occurring randomly. Streamlines plots in Figure 4 (a)-(c) show that the switches correspond to vertical shifts of the flow structure by a half-wavelength $A_z/2$. This symmetry is apparent in the phase portrait (Figure 4 (d)). The disappearance and formation of flow structures at two locations separated by half a wavelength $A_z = 2.5$ is reminiscent of heteroclinic connections between diametrially opposed fixed points in systems with $O(2)$ symmetry. Structurally stable heteroclinic connections between fixed points or periodic solutions have been shown to exist in the systems with $O(2)$ symmetry[16, 17]. However, we are not aware of equivalent theoretical results for heteroclinic connection between strange attractors. As Ra is further increased beyond about $Ra = 13000$, a new periodic regime is observed (Figure 5 (a)). When Ra is further increased to $Ra = 14000$, the temporal behavior of the flow becomes chaotic again, and a new intermittent regime is observed as indicated by the timeseries of Fourier mode $Re(\hat{T}(1))$ in Figure 5 (b).

4 Conclusions

The dynamics of the natural convection of air between two vertical plates maintained at different temperatures have been studied in a domain of small periodic dimensions. Temporal chaos occurs

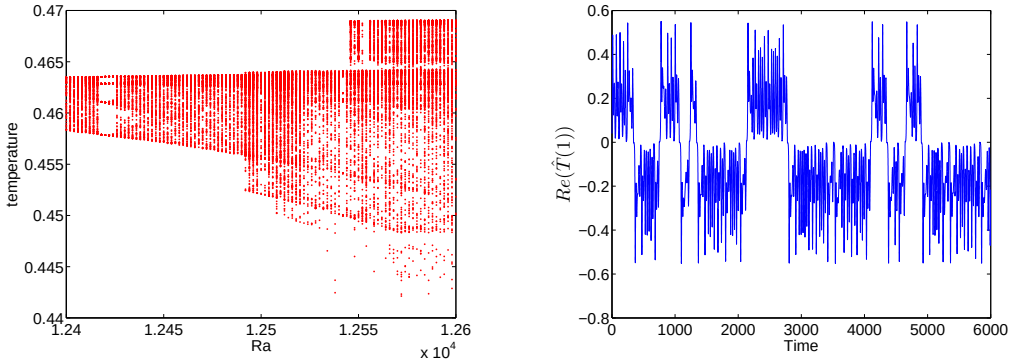

(a) (b)

FIGURE 3 – (a) : Bifurcation diagram for $Ra \in [12400, 12600]$; (b) : Real part of the temporal evolution of the Fourier mode $\hat{T}(k)$ $(k = 1)$ calculated on the line ($x = 0.0381$ and $y = 0.5$), $Ra = 12600$.

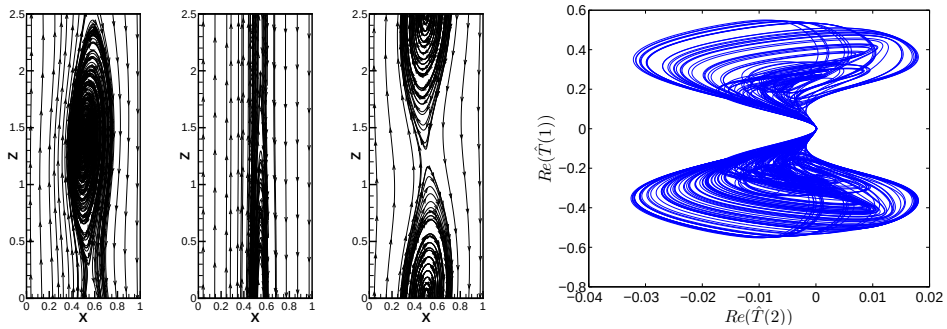

(a) t=8500 (b) t=8525 (c) t=8540 (d)

FIGURE 4 – (a)-(c) : flow streamlines at different instants on the plane $y = 0.5$, $Ra = 12600$; (d) : Phase portraits by temporal evolution of the Fourier modes $\hat{T}(k)$ calculated on the line ($x = 0.0381$ and $y = 0.5$). Abscissa : $Re(\hat{T}(1))$; ordinate : $Re(\hat{T}(2))$.

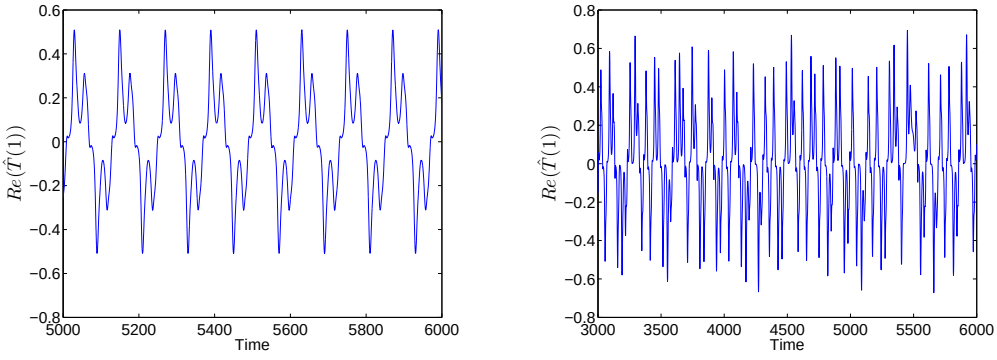

(a) $Ra = 13000$ (b) $Ra = 14000$

FIGURE 5 – Temporal evolution of $Re(\hat{T}(1))$ at two different Ra.

through a sequence of period-doubling bifurcations. In physical space, it corresponds to the modulated pulsation of three-dimensional spatially localized structures, which consist of distorted transverse rolls connected by secondary vortices or braids. Estimations of the Feigenbaum constant from the first few bifurcations are reasonably close to the expected theoretical value. A bifurcation diagram as Ra is increased was constructed for the temperature evolution of a point in the flow. Several features common to the characteristics of one-dimensional maps were identified, such as periodic windows and instances of interior crises. As Ra is further increased, a crisis-induced intermittency is observed, as the structures are shifted vertically by half a wavelength. A periodic window occurs for higher Rayleigh numbers, which then gives way to intermittent, chaotic behavior again. The intermittent behavior observed suggests that heteroclinic connections could be occurring between strange attractors in a system with O(2) symmetry.

Références

[1] Batchelor, G.K. 1954 Heat transfer by free convection across a closed cavity between vertical boundaries at different temperature *Quart. Appl. Math* **12** 209-233

[2] Ruth, D.W. 1979 On the transition to transverse rolls in an infinite vertical fluid layer - a power series solution *Int. J. Heat Mass Transfer* **22** 1199-1208

[3] Bergholz, R.F. 1978 Instability of steady natural convection in a vertical fluid layer *J. Fluid Mech.* **84** 743-768

[4] Chait, A., Korpela, S. 1989 The secondary flow and its instability for natural convection in a tall vertical closure *J. Fluid Mech.* **200** 189-216

[5] Clever, R., Busse, F. 1996 Tertiary and quarternary solutions for convection in a vertical fluid layer heated from the side *Chaos, Soli., Frac.* **5** 163-170

[6] Gao, Z., Sergent, A., Podvin, B., Xin, S., Le Quéré, P. On the transition to chaos of natural convection between two infinite differentially heated vertical plates *Phys. Rev. E* **submitted**

[7] Lizee, A., Alexander, J.I.D 1997 Chaotic thermovibrational flow in a laterally heated cavity *Phys. Rev. E* **56** 4152-4156

[8] Xin, S., Le Quéré, P. 1995 Direct numerical simulation of two-dimensional chaotic natural convection in a differentially heated cavity of aspect ratio 4 *J. Fluid Mech.* **304** 87-118

[9] Paolucci, S., Chenoweth, D.R. 1989 Transition to chaos in a differentially heated vertical cavity *J. Fluid Mech.* **201** 379-410

[10] Janssen, R.J.A., Henckes, R.A.W.M. 1995 Influence of prandtl number on instability mechanismes and transition in a differentially heated square cavity *J. Fluid Mech.* **290** 319-344

[11] Xin, S., Le Quéré, P. 2002 An extended Chebyshev pseudo-spectral benchmark for the 8 :1 differentially heated cavity *Int. J. Num. Meth. in Fluids* **40** 981-998

[12] Eckmann, J.P. 1981 Roads to turbulence in dissipative dynamical systems *Rev. Modern Physics* **53** 643-654

[13] Feigenbaum, M.J. 1980 Universal behavior in nonlinear systems *Los Alamos Sciences* **1** 4-27

[14] Lorenz, E.N. 1963 Deterministic nonperiodic flow *J. Atm. Sci.* **20** 130-141

[15] Grebogi, C., Ott, E., Romeiras, F., Yorke, J. 1987 Critical exponent for crisis-induced intermittency *Phys. Rev. A* **36** 5365-5380

[16] Melbourne, I., Chossat, P., Golubitsky, M. 1989 Heteroclinic cycles involving periodic solutions in mode interactions with O(2) symmetry *Proc. Roya. Soc. Edinburgh : Sec. A Math.* **113** 315-345

[17] Armbruster, D., Guckenheimer, J., Holmes, P. 1987 Heteroclinic cycles and modulated travelling waves in systems with O(2) symmetry *Physica D.* **29** 257-282